Journal of Magnetics 8(4), 142-145 (2003)

X-ray Absorption and Photoemission Spectroscopy Study of $Nd_{1/2}A_{1/2}Mn_{1-y}Cr_yO_3$ (A=Ca, Sr)

J.-S. Kang[1], J. H. Kim[1], S. W. Han[2], K. H. Kim[2], E. J. Choi[3], A. Sekiyama[4], S. Kasai[4], S. Suga[4], and T. Kimura[5]

[1]*Department of Physics, The Catholic University of Korea, Puchon 420-743, Korea*
[2]*Department of Physics, Gyeongsang National University, Chinju 660-701, Korea*
[3]*Department of Physics, The University of Seoul, Seoul 130-743, Korea*
[4]*Department of Material Physics, Graduate School of Engineering Science, Osaka University, Osaka 560-8531, Japan*
[5]*Department of Applied Physics, University of Tokyo, Tokyo 113-0033, Japan*

(Received 23 September 2003)

Valence states and electronic structures of Cr-doped $Nd_{1/2}A_{1/2}MnO_3$ (NAMO; A=Ca, Sr) manganites have been investigated using x-ray absorption spectroscopy (XAS) and high-resolution photoemission spectroscopy (PES). All the Cr-doped NAMO systems exhibit the clear metallic Fermi edges in the Mn e_g PES spectra near E_F. The spectral intensity at E_F is higher for Cr-doped $Nd_{1/2}Sr_{1/2}MnO_3$ (NSMO) than for Cr-doped $Nd_{1/2}Ca_{1/2}MnO_3$ (NCMO), reflecting the stronger metallic nature for NSMO than for NCMO. The measured Cr 2*p* XAS spectra are found to be very similar to that of Cr_2O_3, indicating that Cr ions in Cr-doped NAMO are in the trivalent Cr^{3+} states (t^3_{2g}). The Cr 2*p* XAS data are consistent with the Cr 3*d* PES spectra located at ~1.3 eV below E_F and having no emission near E_F.

Key words : photoemission, XAS, manganite, electronic structure

1. Introduction

$Nd_{1/2}A_{1/2}MnO_3$ (NAMO; A=Ca, Sr) manganites exhibit the charge-ordered (CO), orbital-ordered (OO), and quarter-filled insulating ground states with the CE-type antiferromagnetic (AFM) spin ordering. Doping magnetic impurities at the Mn site, such as Cr and Ru, induce both metallicity and ferromagnetism in the insulating antiferromagnetic NAMO [1-4]. To explain the Cr-induced insulator-to-metal (I-M) transition, the relaxor-ferromagnet has been proposed [4], in which the field-induced I-M transition takes place due to the growth of ferromagnetic (FM) microclusters in a matrix of the CO/OO state. However, this proposal has not been proved.

To understand the origin of the Cr-induced I-M transition in $Nd_{1/2}A_{1/2}Mn_{1-y}Cr_yO_3$, it is important to investigate the valence and spin states of Cr impurities as well as the role of doped Cr ions in the metallic band formation. Photoemission spectroscopy (PES) and x-ray absorption spectroscopy (XAS) [5, 6] provide direct information on the electronic structures of the manganites and the valence states of transition-metal (T) ions, respectively. In our previous study [7], we have investigated the role of the electronic structures of $Nd_{1/2}A_{1/2}Mn_{1-y}Cr_yO_3$ in the I-M transition using the resonant valence-band PES near the Cr and Mn $2p \rightarrow 3d$ absorption edges. It was found that doped Cr ions in NAMO are in the localized trivalent Cr^{3+} states (t^3_{2g} configuration), and that the Cr e_g states are located above the Mn e_g states near E_F. In this paper, we report the Cr 2*p* XAS study of Cr-doped NAMO, in which the valence states of the doped Cr ions are directly observed.

*Corresponding author: Tel: +82-32-340-3382,
e-mail: kangjs@catholic.ac.kr

2. Experimental Details

$Nd_{1/2}A_{1/2}Mn_{1-y}Cr_yO_3$ single crystals (*A*=Ca, Sr; y=0.05, 0.07) were grown using the floating zone method [4]. The valence-band PES and XAS experiments were performed at the undulator beam line BL25SU of SPring-8 equipped with a SCIENTA SES200 analyzer. Samples were fractured and measured in vacuum better than 3×10^{-10} Torr at $T \lesssim 20$ K. PES data were obtained in the transmission mode, with the overall energy resolution

[FWHM: full width at half maximum] of about 80 meV at $h\nu$~600 eV. All the spectra were normalized to the photon flux estimated from the mirror current. All the samples have shown a clean single peak in the O 1*s* core-level spectra and no 9 eV binding energy (BE) peak in the valence-band spectra, which appear when the measured surface is contaminated [8]. XAS spectra were obtained by employing the total electron yield method, and the energy resolution for the XAS data was set at ~100 meV at the Cr 2*p* absorption threshold.

3. Results and Discussion

Figure 1 compares the near-E_F regions of the high-resolution valence-band spectra of Cr-doped $Nd_{1/2}Ca_{1/2}MnO_3$ (NCMO) and $Nd_{1/2}Sr_{1/2}MnO_3$ (NSMO). These data were obtained with the FWHM of $\approx$ 80 meV. As a reference for a typical metal, we present the PES spectrum of Pd which was obtained under the same experimental conditions. $h\nu = 643$ eV (top) corresponds

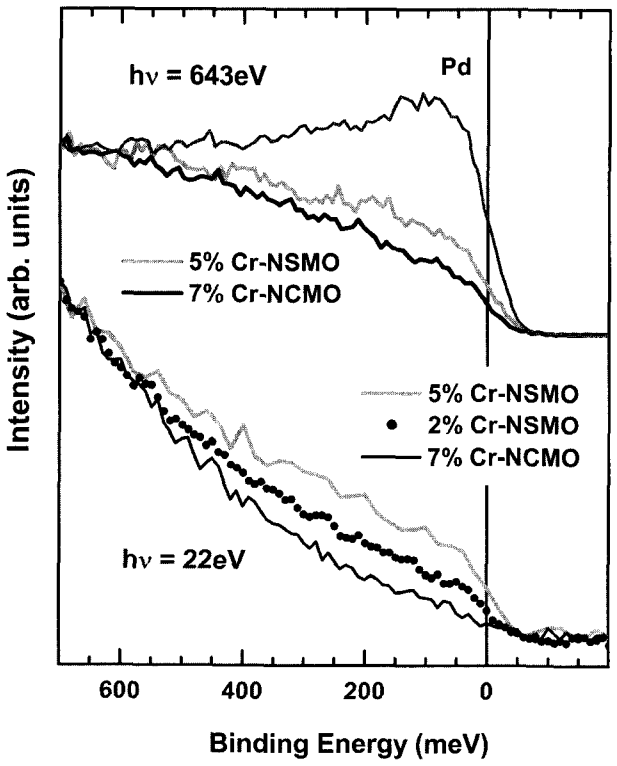

Fig. 1. Top: Near-E_F region of the valence-band spectra of $Nd_{1/2}A_{1/2}Mn_{1-y}Cr_yO_3$ (A=Ca, Sr; y=0.05, 0.07) at the Mn 2*p* $\rightarrow$ 3*d* on-resonance ($h\nu = 643$ eV). These two spectra are scaled at the peak maxima. As a reference for a typical metal, the PES spectrum for Pd is shown, which was obtained at the same $h\nu$ with the same experimental conditions. Bottom: Similarly for $h\nu = 22$ eV. The $h\nu = 22$ eV spectrum of $Nd_{1/2}Sr_{1/2}Mn_{0.98}Cr_{0.02}O_3$ is also presented.

to the on-resonance energy in the Mn 2*p* $\rightarrow$ 3*d* resonant photoemission spectroscopy (RPES) [5]. Note that the previous Cr 2*p* $\rightarrow$ 3*d* RPES study for Cr-doped NAMO [7] has revealed that the Cr 3*d* derived states lie around ~1.3 eV below the Fermi level E_F, and that the electronic states near E_F have no Cr 3*d* character. Hence the $h\nu = 643$ eV spectra can be considered to represent the Mn e_g partial spectral weight (PSW) distributions [9]. On the other hand, the $h\nu = 22$ eV spectra (bottom) reveal very weak spectral intensity near E_F ($I(E_F)$), as compared to $h\nu = 643$ eV. This difference arises from the fact the O 2*p* emissions are dominant at $h\nu = 22$ eV and that the O *p* states have a negligible contribution near E_F [10].

The metallic Fermi edges are clearly observed for both Cr-doped NCMO and Cr-doped NSMO in the Mn e_g PES spectra ($h\nu = 643$ eV), which is consistent with their observed metallic ground states. The spectral intensity near E_F ($I(E_F)$) is proportional to the carrier density at E_F. Note that Cr-doped NSMO exhibits a higher $I(E_F)$ than Cr-doped NCMO and that $I(E_F)$ in Cr-doped NAMO is lower than in Pd. This trend indicates the stronger metallic nature for NSMO than for NCMO and the lower carrier density near E_F in NAMO than in a typical metal. This finding also reveals that the Mn e_g states play an important role in determining the I-M transition in Cr-doped NAMO. Remember that the Cr e_g states are expected not to participate in the formation of the band near E_F [7] nor to affect the bandwidth of the e_g states near E_F [11]. This feature could be understood based on the previous finding that Cr spins order antiparallel to the Mn subnetwork [12], and so the hopping between Cr and neighboring Mn ions is not allowed. This conclusion is supported by the comparison of the Mn e_g PES spectra ($h\nu = 643$ eV in Fig. 1).

Figure 2 compares the Cr 2*p* XAS spectrum of 7% Cr-doped NCMO to that of a reference material Cr_2O_3 having the formally trivalent Cr ions. The latter data has been reproduced from Ref. [13]. In the comparison to Cr_2O_3, the linear background has been subtracted from the XAS spectrum of 7% Cr-doped NCMO. The quality of the Cr 2*p* XAS spectrum of 5% Cr-doped NSMO (not shown here) is not good, but very similar to that of 7% Cr-doped NCMO. The T 2*p* XAS spectrum results from the dipole transitions from the 2*p* core level to the empty 3*d* states, and is dominated by the large Coulomb interaction between the 2*p* core hole and the empty 3*d* levels [14, 15]. Then the peak positions and the line shape of the T 2*p* XAS spectrum depend on the local electronic structure of the T ion, and so they provide the information about the valence state as well as the ground state symmetry of the T ion.

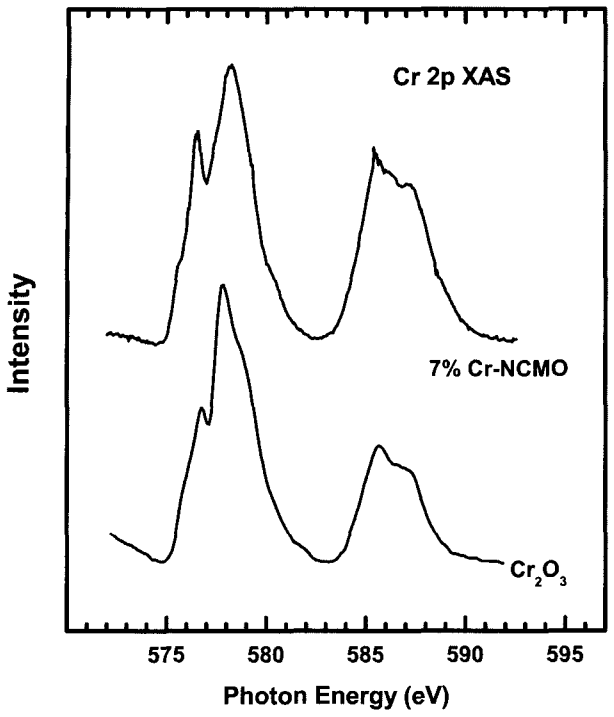

Fig. 2. The Cr 2*p* XAS spectrum of 7% Cr-NCMO, in comparison to that of Cr_2O_3 (Ref. [13]).

Figure 2 clearly shows that the Cr 2*p* XAS spectrum of 7% Cr-doped NAMO is very similar to that of a formally trivalent Cr_2O_3, indicating that Cr ions in Cr-doped NAMO are in the trivalent valence states: Cr^{3+} (t_{2g}^3). This finding in XAS is consistent with the previous finding of PES [7] that the Cr 3*d* states are located around ~1.3 eV below E_F, with no Cr 3*d* states near E_F. Therefore the Cr 2*p* XAS spectra of Cr-doped NAMO suggest that Cr e_g states do not participate in the formation of the band near E_F.

The mechanism of the I-M transition in Cr-doped NAMO may be understood based on our observations, as discussed below. We have found that Cr ions in $Nd_{1/2}A_{1/2}Mn_{1-y}Cr_yO_3$ are in the trivalent Cr^{3+} state (t_{2g}^3) and that the Cr t_{2g} states are located well below E_F. Then the substitution of a Cr^{3+} (d^3) for a Mn^{3+} (d^4) site in the CO/OO NAMO will correspond to the hole filling in the undoped NAMO. Since the undoped CO/OO NAMO is expected to have the ordered Mn^{3+}/Mn^{4+} ($3d^4/3d^3$) configuration [16, 17], the doped Cr^{3+} ion will play a role similar to the substitution of a Mn^{4+} ion for a Mn^{3+} ion. So one can simply conjecture that these extra carriers, caused by the impurity doping, break the commensurate quarter-filled CO/OO state and transform the CO/OO insulating phase into the metallic phase. This conjecture is consistent with the phase diagram of NSMO, where the CO/OO insulating AFM phase of half-doped NSMO is transformed into the metallic AFM phase with increasing the hole concentration [16].

Here we would like to mention that a Cr^{3+} ion itself does not participate in the double-exchange (DE) mechanism in the metallic phase. This is because two configurations of Mn^{3+}-Cr^{3+} and Mn^{4+}-Cr^{2+} are not degenerate, as observed in the PES above (See Fig. 1). The doped Cr^{3+} ions would just initiate the hopping of carriers in the system. However, the above picture of the filling control is not complete since the NCMO-based system, which is the stronger CO system, would not exhibit the metallic phase merely with the filling control. Hence it is likely that not only the valence state but also the spin state and the electronic structure are important.

4. Conclusions

In conclusion, the valence states and the electronic structures of Cr-doped NAMO (A=Ca, Sr) have been investigated by employing XAS and PES using synchrotron radiation. All the Cr-doped NAMO systems exhibit the clear metallic Fermi edges in the Mn e_g spectra near E_F, consistent with their metallic ground states and the unoccupied Cr e_g states. The spectral intensity at E_F is higher for the NSMO-based system than for the NCMO-based system. The Cr 2*p* XAS spectra of Cr-doped NAMO are found to be very similar to that of a formally trivalent Cr_2O_3, indicating that Cr ions in Cr-doped NAMO are in the trivalent Cr^{3+} (t_{2g}^3) states. This finding in XAS is consistent with the finding of PES that Cr 3*d* states are located at ~1.3 eV below E_F, and suggests that Cr e_g states do not participate in the formation of the band near E_F. Our measured electronic structures for Cr-doped NAMO are consistent with the concept of the hole filling for the origin of the Cr-induced ferromagnetism and I-M transitions.

Acknowledgments

This work was supported by the KRF (KRF--2002-070-C00038) and in part by the Catholic University of Korea (20030219). PES experiments were performed at the SPring-8 (JASRI: 2001B0028-NS-np).

References

[1] B. Raveau, A. Maignan, and C. Martin, J. Solid State Chem. **130**, 162 (1997).
[2] A. Barnabé, A. Maignan, M. Hervieu, F. Damay, and B. Raveau, Appl. Phys. Lett. **71**, 3907 (1997).
[3] Y. Moritomo, A. Machida, S. Mori, N. Yamamoto, and

A. Nakamura, Phys. Rev. B **60**, 9220 (1999).
[4] T. Kimura, Y. Tomioka, Y. Okimoto, and Y. Tokura, Phys. Rev. Lett. **83**, 3940 (1999); T. Kimura, R. Kumai, Y. Okimoto, Y. Tomioka, and Y. Tokura, Phys. Rev. B **62**, 15021 (2000).
[5] A. Sekiyama, S. Suga, M. Fujikawa, S. Imada, T. Iwasaki, K. Matsuda, K. V. Kaznacheyev, A. Fujimori, H. Kuwahara, and Y. Tokura, Phys. Rev. B **59**, 15528 (1999).
[6] J.-S. Kang, J. H. Kim, A. Sekiyama, S. Kasai, S. Suga, S. W. Han, K. H. Kim, T. Muro, Y. Saitoh, C. Hwang, C. G. Olson, B. J. Park, B. W. Lee, J. H. Shim, J. H. Park, and B. I. Min Phys. Rev. B **66**, 113105 (2002).
[7] J.-S. Kang, J. H. Kim, A. Sekiyama, S. Kasai, S. Suga, S. W. Han, K. H. Kim, E. J. Choi, T. Kimura, T. Muro, Y. Saitoh, C. G. Olson, J. H. Shim, and B. I. Min Phys. Rev. B **68**, 012410 (2003).
[8] T. Saitoh, A. E. Bocquet, T. Mizokawa, H. Namatame, A. Fujimori, M. Abbate, Y. Takeda, and M. Takano, Phys. Rev. B **51**, 13942 (1995).
[9] J.-H. Park, C. T. Chen, S.-W. Cheong, W. Bao, F. Meigs, V. Chakarian, and Y. U. Idzerda, Phys. Rev. Lett. **76**, 4215 (1996).
[10] J.J. Yeh and I. Lindau, *At. Data Nucl. Data Tables* **32**, 1 (1985).
[11] S. J. Youn and B. I. Min, J. Korean. Phys. Soc. **32**, 576 (1997).
[12] O. Toulemonde, F. Studer, A. Barnabé, and J. B. Goedkoop, J. Appl. Phys. **86**, 2616 (1999).
[13] C. Theil, J. van Elp, and F. Folkmann, Phys. Rev. B **59**, 7931 (1999).
[14] F. M. F. de Groot, J. C. Fuggle, B. T. Thole, and G. A. Sawatzky, Phys. Rev. B **42**, 5459 (1990).
[15] G. van der Laan and I. W. Kirkman, J. Phys.: Condens. Matter **4**, 4189 (1992).
[16] J. van den Brink and D. Khomskii, Phys. Rev. Lett. **82**, 1016 (1999).
[17] B. I. Min, Y.-K. Jo, M.-S. Kim, Physica B **312**, 723 (2002).